Interfacial roughness correlation in multilayer films: Influence of total film and individual layer thicknesses

D. E. Savage, N. Schimke, Y.-H. Phang, and M. G. Lagally
Department of Materials Science and Engineering, University of Wisconsin-Madison, Madison, Wisconsin 53706

(Received 28 October 1991; accepted for publication 28 December 1991)

A series of W/C multilayer films sputter deposited on Si(100) substrates with total thickness ranging from 400 to 6400 Å and bilayer period from 20 to 160 Å were examined to explore the variation of interfacial roughness and interfacial roughness correlation with film thickness and period. The films were characterized with x-ray diffractometry. Average interfacial roughness is obtained from conventional $(\theta,2\theta)$ scans, while information on roughness correlation is extracted from rocking-curve (transverse-profile) analysis. The magnitude of the roughness is found to depend more on bilayer period than on total film thickness. The observations suggest that interfaces retard the evolution of surface roughness and that thin "restarting" layers may be used to control the growth morphology of thin films.

I. INTRODUCTION

Control of interfacial roughness and its correlation from interface to interface in multilayer thin films is of both practical and fundamental interest. Film properties that depend on the quality of individual interfaces or that depend on the overall perfection of the artificial one-dimensional crystal (multilayer film) will be controlled by the interfacial quality. Knowledge of the interfacial roughness, i.e., its magnitude, its lateral length scale (wavelength), and the relationship of roughness at one interface to that at subsequent interfaces, will lend insight into the fundamental processes involved in film growth and is needed if one is ultimately to control roughness in multilayer devices.

Interfacial roughness has technological applications in many multilayer systems, e.g., magnetic multilayers, semiconductor multilayers for electron transport or light-emitting devices, or x-ray optical elements. For semiconductor materials, interfacial roughness affects both electrical and optical properties. Here, it is of particular interest to know the lateral scale of the interfacial roughness because, for a given amount of roughness, the effect on both the electrical and optical properties will depend on its wavelength. For magnetic multilayers, a precise knowledge of interfacial roughness is needed to understand details of long-range magnetic coupling. For soft-x-ray optical elements, reduction of interfacial roughness is crucial. It is well known that interfacial roughness attenuates the specular reflectivity from multilayer soft-x-ray mirrors.[1] In addition, correlated roughness, i.e., that which is replicated from the initial substrate through the subsequently deposited layers, will cause diffusely scattered radiation to be concentrated in a halo around the specular beam. This "figure-error" will limit the contrast for imaging applications.[2] This paper concentrates on the type of material combinations suitable for these x-ray optical elements, and in particular W/C films. A future publication will concentrate on semiconductor multilayers.[3]

Traditional methods used to study interfacial roughness in multilayer films include x-ray diffraction (XRD) and cross-sectional transmission electron microscopy (CTEM). The average interfacial roughness can be inferred from XRD measurements of the integrated specular reflectivity as a function of the angle of incidence or the wavelength. Measurements of the specular reflection give no information on how roughness is correlated. High-resolution CTEM gives details or the structure of individual interfaces on the microscopic scale, including evidence for interdiffusion and chemical reaction. However, information on the magnitude of interfacial roughness on length scales shorter than the film's cross section is lost due to averaging inherent in transmitting through the film.[4] This averaging also limits the technique's ability to study roughness correlation from interface to interface. There is additionally the possibility that artifacts may arise in the cross-sectioning of a sample.[5]

Information on roughness correlation can be obtained from measurements of the angular distribution of diffusely scattered x rays. We have outlined methods by which such information can be obtained and interpreted.[6] In the present work we use these methods to analyze the influence of several growth parameters on interfacial roughness. We study a series of W/C multilayers deposited on Si(100), varying independently the total film thickness and the individual layer spacings. In addition, we examine the effect of an initial carbon "buffer" layer, which has been suggested as a smoothening layer.[7]

The outline of this paper is as follows. In Sec. II, we briefly review aspects of surface and interfacial roughness and their relation to film growth. In Sec. III, we provide details of the experiment, followed by a summary of the theory required to analyze the data in Sec. IV, results in Sec. V, a discussion of the implications in Sec. VI, and a brief conclusion in Sec. VII.

 0021-8979/92/073283-11$04.00

II. SURFACE AND INTERFACIAL ROUGHNESS: A BRIEF REVIEW

The evolution of surface roughness during growth is by definition a nonequilibrium process, i.e., one must have a supersaturation of vapor in order for a film to grow. Because of this, surface roughness will be determined in part by kinetic limitations, a competition between various rates. Other factors will also be important, including the initial substrate roughness and chemical reaction between adspecies and substrate.

Interfacial roughness is related to surface roughness in that the same kinetic limitations are present during the growth of an individual layer as in a single film. In the simplest case, with no chemical reaction or interdiffusion between layers, the interfacial roughness of a given layer is simply the surface roughness of a film with the thickness of the individual layer deposited on a substrate with the roughness of the previous layer.

A. Single-layer roughness

For single-layer thin films, surface roughness is expected to depend on the total film thickness.[8] For films deposited close to equilibrium conditions, the film morphology at steady state is ideally independent of initial substrate morphology but reflects only the competition of different kinetic processes. In the simplest example, the evaporative deposition of a material onto an initially perfect single-crystal substrate of the same material, roughness arises from the competition between the arrival rate of the deposited species and its diffusion rate.[9] In this case, roughness can only increase or reach some steady-state value as, for example, in the molecular-beam epitaxy (MBE) growth of Si on Si. If, on the other hand, the substrate is initially rough, smoothening can initially occur as is observed for MBE grown GaAs on GaAs(100).[10] For such a system, the lateral diffusion length of the deposited species is larger than the initial lateral length scale of the substrate roughness, allowing depressions to be filled in. The steady-state morphology is again determined by the competition between arrival and diffusion rates: the roughness may be low or high although the morphology is generally smoother than the initial surface. Such films are called buffer layers.

If films are deposited at conditions far from equilibrium, film morphology for evaporated films is described qualitatively in terms of three zones depending on the ratio T/T_M, where T is the substrate temperature and T_M is the deposited material's melting temperature.[11] A transition zone between zones 1 and 2 is added in order to describe sputter-deposited films.[12] The effect of pressure is also included, with films grown at higher pressures having more porous structures. The morphology for growth in zone 1, $T/T_M \leqslant 0.3$, is characterized by a columnar fine-grain microstructure. In zone 2, T/T_M between 0.3 and 0.5, columns are larger due to increased surface diffusion. Finally in zone 3, $T/T_M \geqslant 0.5$, there is sufficient mobility for grains to recrystallize and the columnar structure is lost. For growth in zones 1 and 2 shadowing by raised regions of the film can also contribute to the evolution of roughness.[13]

Studies of surface morphologies of films grown in conditions in zone 1, with the deposit incident normal to the substrate, show a self-similar behavior, i.e., film morphology appears similar over many orders of magnitude of magnification. Eventually, however, at low enough magnification, the film will appear smooth. In other words, there is a maximum roughness wavelength, which has been found to scale with film thickness. For example, for the growth of pyrolytic graphite the lateral scale of the roughest features, i.e., the roughness with the longest wavelength, was found to increase as $t^{0.75}$, where t is the film thickness.[14] Such behavior has been predicted by a range of growth models.[8,15,16] In such models the local lateral scale of the roughness, ξ, increases initially as $\xi \propto t^{\alpha}$ and the local width of the interface region, w, increases as $w \propto t^{\beta}$. Here β is the growth exponent and α is an exponent that characterizes the roughness for surface roughness that is described as self-affine. For these models, α is typically $\frac{1}{2}$ and β ranges from $\sim \frac{1}{4}$ to $\frac{1}{2}$.

B. Multilayer roughness

How might this picture change for a multilayer system? Consider a film comprised of alternate layers of materials A and B. In the limit that A and B are indistinguishable as far as the growth process is concerned, one would expect the interfacial roughness to scale with the number of layers deposited in the same way as surface roughness scales with film thickness. If, as is more likely, A and B have different growth behaviors, the situation becomes more complicated. As each layer is deposited, a species must first nucleate on a substrate of the opposing species or, for amorphous films, diffuse along that substrate until a favorable sticking site is found and then, as the substrate fills in, grow on itself. Interdiffusion or chemical reaction between the species may also occur.

The interfacial roughness in an A/B combination may be controlled by some intrinsic property such as an interfacial reaction between the two species. If this were true, the interfacial roughness would be relatively independent of the bilayer period. An interfacial roughness that is relatively independent of bilayer period has been suggested as the reason short-period x-ray mirrors are inefficient reflectors. If the interfacial roughness is a constant independent of layer thickness, it would make a proportionately greater contribution to the individual layer thickness for short-period films and thus affect their reflectivity more than it would that of thicker films. A second possibility is that interfacial roughness is controlled by the evolution of individual layer morphologies. If so, the bilayer period should have a strong effect. This latter possibility is supported by evidence that individual-layer grain size and crystallinity depend strongly on the layer thickness. Both of these possibilities allow for different roughness of the A/B and B/A interfaces. Finally, each layer must be grown on the outer surface of the prior layer deposited, and not on an ideally smooth substrate. Each of these surfaces will have some roughness. It is here that the question of roughness correlation arises, i.e., how is the roughness of one interface related to that of the next?

C. X-ray optical multilayers

Work characterizing the structure and roughness of multilayers suitable for soft x-ray optical applications has focused on the microstructure of the layers themselves, the uniformity in thickness, the rms roughness of the interfaces, and the contribution of reacted zones to roughness.[17] Much of this work has been on W/C multilayers. The conclusions relevant to our present study are discussed here. For sputter deposited films, individual layers of W and C within a multilayer film are found to be "amorphous" for layer thicknesses below ~40 Å. These films are grown at temperatures less than 1/10 of their melting points and at pressures sufficiently low that their expected growth morphology is in zone 1 or in the transition region between zones 1 and 2. Thus, an amorphous or fine polycrystalline structure is expected. Below a mean deposition thickness of 8 Å, W has been found to grow as discontinuous layers,[5] implying the formation of amorphous three-dimensional (3-d) clusters. For layer thicknesses greater than ~40 Å the W layer is found to be microcrystalline.[5,18,19] These results indicate that W atoms have some mobility in films at these deposition temperatures.

The structure of interfaces has been studied with several techniques. Results using high-resolution CTEM imaging and electron diffraction on magnetron sputter deposited W/C films grown on Si(100) show evidence for interfacial roughness replicated through the film.[20] The replicated roughness was more evident in areas of the sample that were the thinnest in cross section. Interfaces appeared smoother in thicker areas due to averaging through the sample. Petford-Long *et al.*,[21] also using high-resolution CTEM on ion beam deposited films, found evidence for different structure in alternate interfaces. They observed that the W-on-C interface was significantly rougher than the C-on-W one and contained crystallites of WC. This is in apparent contradiction with *in situ* ellipsometry and grazing x-ray diffraction results on rf-sputter deposited W/C films, which suggest that the W-on-C interface is abrupt while the C-on-W one is diffuse, containing an interdiffused 4 Å region.[22]

The thickness dependence of the crystallization of W layers supports the proposition that the individual-layer thickness has a strong influence on layer morphology and consequently interfacial roughness. In light of this dependence, it is not surprising that alternate interfaces may have different amounts of roughness.

III. EXPERIMENT

In this section we outline details of sample preparation, followed by a discussion of the diffraction apparatus used to characterize the films. We give specific details on the different diffraction geometries used to extract interfacial roughness and interfacial roughness correlation.

A. Deposition

Multilayer films were deposited in a dc magnetron sputter deposition system with a base pressure of 3×10^{-7} Torr. Substrates were loaded on a rotary table and passed alternately over C and W sources. The sputtering gas was Ar with a partial pressure during deposition of 5 mTorr. Deposition is nominally at room temperature, although the substrates may reach 100 °C for some deposition conditions. The resultant growth rates, with the table stationary, were 0.9 and 1.8 Å/s for C and W respectively. Layer thicknesses were controlled by varying the table speed. For all samples, the C and W layer thicknesses were chosen to be approximately equal. The Si(100) wafers used for substrates were prepared by rinsing in ethanol. Other treatments such as oxide removal with subsequent reoxidation were found to give rougher substrates.

To examine the effect of film thickness on interfacial roughness, a series of films with a 40-Å bilayer period was deposited, varying the number of bilayers, N. We chose values of $N = 10$, 20, 40, 60, 80, and 160.

In a separate set of depositions samples were grown with bilayer periods, d, of 20, 40, 80 and 160 Å, fixing the number of layer pairs deposited at $N = 40$. Here the thickness of the sample is changing with the period but comparisons can be made with films of equal thickness with a 40-Å period from samples in the first set of depositions. In addition, samples with $N = 10$ and a 160-Å period were produced to compare directly with the $N = 40$, $d = 40$ samples.

Finally, films with an initial 500-Å carbon layer followed by an $N = 40$, $d = 40$ multilayer film were deposited to examine the influence of carbon as a smoothening layer. Also a film with an initial 20-Å W layer followed by a 400-Å C buffer layer, and an $N = 40$, $d = 40$ multilayer was prepared to test whether an initial W wetting layer is useful.

B. X-ray diffraction measurements

Measurements of the specular intensity versus angle of incidence and measurements of the distribution of the diffusely scattered intensity around the maximum in the specular intensity (the integral diffraction orders satisfying Bragg's law) were used to determine the magnitude of the interfacial roughness and the degree of interfacial roughness correlation. The measurements were carried out using a conventional two-circle x-ray diffractometer. The angle between the source and sample (ω) and the angle between the source and detector (2θ) can be varied independently and are stepper motor controlled to an accuracy of 0.001°. The source is a Cu $K\alpha$ x-ray tube and the detector incorporates a graphite monochromator set to detect Cu $K\alpha$ radiation. The source is defined by slits of 0.03° width within the plane of diffraction while the detector aperture slits are set to subtend an angle of 0.01°. Relative intensities are determined by normalizing to the primary-beam intensity.

Three different types of measurements were made: conventional (θ,2θ) scans, rocking-curve scans (with a narrow detector aperture, sometimes called transverse-profile scans) and offset-(θ,2θ) scans. Each probes the intensity of scattered x rays in different cuts through reciprocal space. In the (θ,2θ) geometry, the portion of the specularly scat-

tered intensity subtended by the detector is measured as the incidence angle is varied. The size of the detector can be varied to include more or less intensity, but the conventional measurement is with a wide detector, so that an integral intensity is measured. This is, of course, a cut through reciprocal space normal to the surface. The rocking curve is made by rocking the sample, varying ω, while holding the source and the detector fixed. In this measurement the detector aperture is small so that the scattered intensity along a radial cut with radius equal to the magnitude of the momentum transfer vector, $|\mathbf{S}| = 4\pi \sin(\theta)/\lambda$, is sampled. For small rocking angles, the diffracted-beam intensity distribution parallel to the surface is obtained. Offset-$(\theta,2\theta)$ scans are accomplished by collecting a $(\theta,2\theta)$ curve with the sample intentionally misaligned by a small angle. The resultant cut in reciprocal space is nearly normal to the surface. It probes the distribution of the diffusely scattered intensity normal to the surface while missing the contribution from the strong Bragg peaks.

IV. THEORY AND DATA ANALYSIS

In this section we review the methods used to extract interfacial roughness and roughness correlation from the x-ray diffraction measurements and illustrate them with an example. Modeling the intensity scattered in the specular direction gives information about the average multilayer structure normal to the surface. The location of diffracted peaks gives, of course, the film period. The average structure of a bilayer pair then modulates the intensity of these maxima in an analogue to the single-slit envelope function for a 1-d diffraction grating. By examining the modulation various details about the average bilayer structure can be inferred. The ratio, Γ, of the W layer thickness to the film period thickness determines the periodic modulation of peak intensities. Interfacial roughness appears as an overall reduction of intensity, with higher orders being reduced preferentially. Additional information on bilayer structure, i.e., the difference in roughness in alternate B/A, A/B interfaces can also be obtained and will be discussed later.

While the magnitude of the average interfacial roughness can be obtained from the specular intensity, no information is gained on how it is correlated. It is by probing the spatial distribution of the diffusely scattered intensity that information on both lateral and vertical roughness correlation can be inferred.

A. Specular reflectivity

The $(\theta,2\theta)$ scans show the decay of intensity with diffraction order that is typical of such measurements. Measurements are fit using a recursion approach.[23] Initially, we assume that all interfaces in a multilayer film are equally rough. The outcome of the fitting is then the root mean square (rms) interfacial roughness, σ, which can also be thought of as the interface width. The value obtained will depend on the choice of the functional form of the interfacial roughness used in the model. For example, given an interface with a Gaussian distribution of interfacial heights, the probability, $P(h - \langle h \rangle)$, of finding the height, h, different from the average interfacial height, $\langle h \rangle$, is

$$P(h - \langle h \rangle) = \frac{1}{\sigma\sqrt{2\pi}} \exp \frac{-(h - \langle h \rangle)^2}{\sqrt{2}\sigma^2}. \quad (1)$$

With this assumption for the interfacial roughness distribution, the resultant intensity (in the kinematic limit) has a dependence on the magnitude of the rms roughness, σ, that is identical to the well known Debye–Waller attenuation of intensity in thermally excited systems,

$$I(\mathbf{S}) = I_0 \exp(-S_z^2\sigma^2), \quad (2)$$

where $\mathbf{S}$ is the momentum transfer vector, $S_z = 4\pi(\sin\theta)/\lambda$ is its component perpendicular to the surface, and σ can be identified as the static equivalent of the vibrational amplitude $\langle u^2 \rangle$. In other words, $(\theta,2\theta)$ scans will show an attenuation with diffraction order that reflects a "static Debye–Waller factor".

Functional forms of interfacial roughness different from the Gaussian of Eq. (1) will give rise to a different attenuation of the specular intensity with diffraction order, but otherwise the treatment is identical.[24] For different functional forms, a fit to experiment produces different values of the interfacial roughness. The more appropriate the functional form is to the actual roughness, the better the fit will be for all diffraction orders.

In a real system it is unlikely that successive interfaces are identically rough. During growth, roughness may build up or decay as additional layers are deposited. At grazing geometry the sampling depth for a $(\theta,2\theta)$ scan will increase significantly with diffraction order. If roughness increases during growth, the first order will be preferentially attenuated because it originates from near the top of the film where roughness is greatest.

There is no reason to believe that the growth of W on C should give the same interfacial roughness as the growth of C on W. The possibility of unequal roughness in alternate interfaces is explored in a later section.

B. Diffuse reflectivity

All W/C multilayers that were examined show a measurable diffusely scattered halo concentrated around the Bragg reflections of the multilayer, indicating the presence of roughness correlated vertically from interface to interface through the film.[6] The spatial distribution of the diffuse intensity is obtained through a combination of transverse (rocking) scans and offset-$(\theta,2\theta)$ scans. These scans are analyzed the extract both lateral and vertical roughness correlation.

We begin by considering vertical roughness correlation. Figure 1 shows both a conventional and an offset-$(\theta,2\theta)$ scan through the 2nd and 3rd orders of a W/C multilayer. An offset angle of 0.5° insures that only diffuse intensity is probed in the offset scan. Both curves show peaks at the multilayer Bragg conditions with essentially the same shapes, a signature of vertically correlated roughness (Ref. 6 can be consulted for a discussion of the essentials of the measurement). The off-specularly scattered ra-

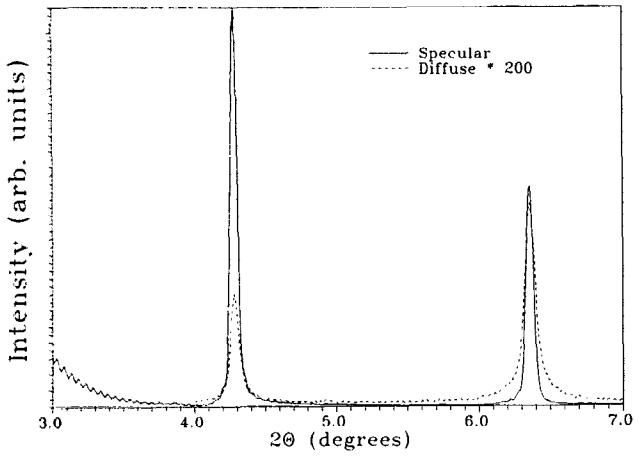

FIG. 1. Comparison of a $(\theta,2\theta)$ scan (solid) through the 2nd and 3rd orders of an $N = 40$, $d = 40$ Å W/C mutlilayer with an offset-$(\theta,2\theta)$ scan (dashed, times 200) through the same range, where the offset angle, $\Delta\omega = 0.5°$. Both scans show peaks at the Bragg conditions. The offset scan probes the distribution of the diffusely scattered radiation nearly normal to the surface; hence the observation that the peaks in the offset scan have approximately the same shapes as in the specular scan shows the presence of vertically correlated roughness.

diation from different interfaces interferes constructively at these conditions. We also note that the intensity of the diffusely scattered radiation increases with increasing order relative to the specular-beam intensity. This behavior is expected because roughness attenuates the specular-beam intensity increasingly with increasing order, redistributing the intensity into the diffuse background.

If interfacial roughness had been uncorrelated from interface to interface, the diffuse intensity would have been distributed in reciprocal space uniformly normal to the surface and not concentrated at the Bragg conditions. The measured peak intensity of the diffuse component would be reduced because it would be distributed over a much larger volume in reciprocal space. We do not rule out the possibility that such a component of roughness is present in addition to the vertically correlated roughness, but its contribution to the diffuse intensity in the plane of the Bragg condition is negligible for the films examined. Another possibility is that roughness is only partially correlated from layer to layer. Differences from perfect vertical correlations will show up in differences in the shape of the offset curve compared with that of the specularly diffracted beam (i.e., differences in the shapes of the curves in Fig. 1).[25] As mentioned these are small in the W/C samples in this investigation.

From the above discussion it is justified to treat the diffuse intensity in the transverse scans as arising from vertically correlated roughness. This allows for a simplified analysis of the transverse scan by reducing it to what is essentially a surface roughness problem.

The procedure for fitting the transverse scans has been described previously.[6] We treat the multilayer interfacial roughness as a structure factor modulating the intensity of a perfect multilayer stack. The structure factor is generated by considering the scattering from a single interface, e.g., a vacuum-surface interface. A rough surface can be characterized by specifying a height-height correlation function. We follow the approach of Sinha *et al.*[26] by using a trial function, calculating the resultant transverse profile, and comparing with a measured curve. We assume that surface roughness is isotropic. The form of the correlation function is chosen as

$$\langle h(r-R)h(r)\rangle = \sigma_{\rm corr}^2 \exp[-(|R|/\xi)^{2\alpha}], \qquad (3)$$

where $\sigma_{\rm corr}$ is the rms value of the vertically correlated roughness, ξ is the lateral correlation length, and α is a fraction between 0 and 1 that is related to the fractal dimension of the surface.[27] This form of correlation function results from treating a surface as locally rough but having an rms roughness independent of the probe size for distances much greater than the correlation length. It is equivalent to treating roughness as self-affine for small separations, but with a roughness cutoff for larger distances.[26] This means that the average surface plane is well defined and unchanging over these same distances. For fractal or self-affine roughness at all dimensions the rms roughness will increase with the area probed. The angular distribution of the intensity scattered from a surface with cutoff roughness can be separated into a sum of two parts, an instrument-limited beam in the specular direction, and a diffuse background. For surfaces with unbounded roughness, the scattered intensity cannot be separated in this way.[26]

Because our measurements are made on a diffractometer with slits sufficiently long to integrate over the diffuse peak in the direction along the slits, we must integrate that intensity along the same direction in our model calculations. For a choice of $\alpha = \frac{1}{2}$ and integrating over S_y, the scattered intensity can be solved analytically and written as[28]

$$\int I(\mathbf{S})dS_y = 2\pi I_0 \exp(-S_z^2\sigma_{\rm corr}^2)\Big/S_z^2\Big(2\pi\delta(S_x) + \sum_{n=1}^{\infty}\frac{2\xi(S_z^2\sigma_{\rm corr}^2)^m}{m(m!)}\frac{1}{(1+S_x^2\xi^2/m^2)}\Big). \qquad (4)$$

To fit with experiment, the model curve must be convolved with a function representing the broadening due to the instrument. In addition, other corrections are needed that take into account the 3-d nature of the scattering problem.[6] One is the correction for the changing pathlengths x rays travel in the sample. X rays are more strongly absorbed at the extremes of the rocking curve, reducing the scattered intensity at these angles. A second correction is for the cut through reciprocal space, which is radial and so not strictly parallel to the Bragg plane. Both of these effects cause the diffuse component of the transverse scan to appear more peaked than would be predicted using Eq. (4). The effect due to absorption is the stronger but is lessened for transverse scans of higher diffraction orders. A third correction is for the changing area of the incident x-ray beam on the

sample. Transverse scans plotted in reciprocal units, e.g., Figs. 3, 6, and 8, have been normalized to the incident-beam area.

The method outlined above is used to fit the shape, but not the absolute intensity, of the transverse scan. A knowledge of the influence of the various parameters on the calculated profile shape allows one to find an optimal fit rapidly. For a given S_z, the ratio of the integrated intensity in the central peak to that of the diffuse background will depend only on the value of the σ_{corr} and can be written

$$\frac{\int I(\mathbf{S})_{\text{spec}}\, dS_x dS_y}{\int I(\mathbf{S})_{\text{diffuse}}\, dS_x dS_y} = \frac{\exp[-(\sigma S_z)^2]}{\{1-\exp[-(\sigma S_z)^2]\}}. \tag{5}$$

The width of the diffuse peak is inversely related to the lateral correlation length. Thus, a sample with a relatively short-wavelength interfacial roughness will have a wider diffuse component than a sample with a longer-wavelength roughness. The shape of the diffuse component will depend on the power spectrum of the interfacial roughness, which is reflected in α. As α is reduced from 1 intensity is distributed more to the wings of the diffuse component while keeping its width relatively unchanged.

We have discussed how the average interfacial roughness can be obtained from measurement of the specular reflectivity and how both the magnitude and lateral correlation length of the vertically correlated roughness can be obtained from the transverse scans. This information can finally be used to estimate the magnitude of vertically random roughness using the relationship[6]

$$\sigma^2_{\text{random}} = \sigma^2_{\text{total}} - \sigma^2_{\text{corr}}. \tag{6}$$

V. RESULTS

We will discuss the results of the measurements in three sections. The first is concerned with the effect of total film thickness, the second with individual-period thickness, and the third with the effect of a carbon buffer layer.

Our main interest here is in examining changes in the roughness from sample to sample. Thus, the various simplifying assumptions used in the model, i.e., that the interface width can be described with a Gaussian distribution and that the average interfacial roughness is not varying with sample depth, should not be a limiting factor. For example, even if roughness is changing throughout the thickness of a film, comparing scans taken with similar geometries from different samples will show relative differences between them.

A. Roughness versus number of layers

In Fig. 2, we show a series of $(\theta,2\theta)$ scans and theoretical fits from films in which d is nominally 40 Å and N is 10, 40, and 160. No single value of σ_{tot} fits all orders. Typically, a larger σ_{tot} is needed to fit the lowest orders. We fit higher orders preferentially. This was done for several reasons. First, the values of the higher orders are much more sensitive to the roughness. By comparing them, differences from sample to sample show up more readily. Second, fitting to the higher orders overestimates the intensity of the first order by 10 to 20%, which can be caused

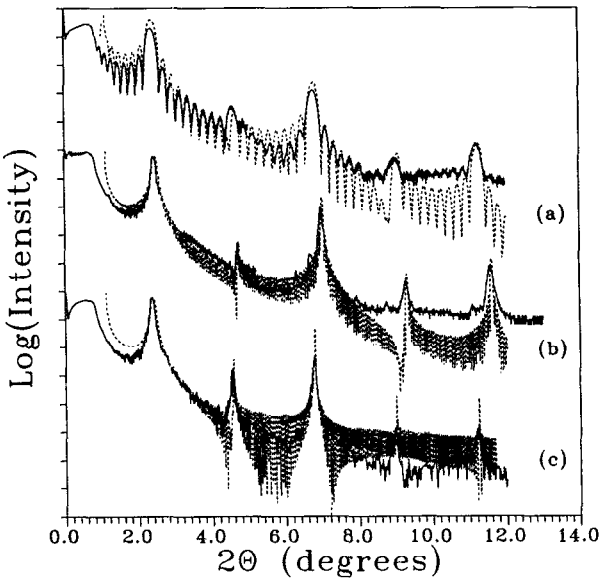

FIG. 2. A series of $(\theta,2\theta)$ scans and theoretical fits (dashed lines) for samples with a nominal period of 40 Å and a varying number of bilayers. (a) $N = 10$, fit parameters: $d = 39.4$ Å, $\Gamma = 0.51$, and $\sigma_{\text{tot}} = 2.7$ Å. (b) $N = 40$, fit parameters: $d = 38.2$ Å, $\Gamma = 0.52$, and $\sigma_{\text{tot}} = 2.7$ A. (c) $N = 160$, fit parameters: $d = 38.9$ Å, $\Gamma = 0.51$, and $\sigma_{\text{tot}} = 3.4$ Å. Note that five diffraction orders are visible in each scan, showing that roughness is varying only slightly with N. The theoretical curves were made assuming equal roughness in all interfaces.

by other factors, while fitting the first order preferentially predicts intensities for the highest orders that are too low by orders of magnitude. There are several possible causes for a reduction in intensity of the first order, including long-range waviness of the sample beyond the limits of resolution of the diffractometer, preferential outer-surface roughness, or an increasing roughness with thickness. The first two possibilities reduce the first-order intensity while affecting the higher-order intensities only slightly. Fitting preferentially to the higher orders would in these cases reflect more accurately the true interfacial roughness. Even if the last possibility is the cause of the reduction of the first-order intensity, the roughness values extracted from the fitting are still useful for comparisons between films. The roughness can be thought of as representing an average roughness over the volume sampled, which is different for each diffraction order. The volume sampled can be estimated using the linear adsorption coefficients for W and C, and calculating the film thickness that will attenuate x rays scattered from an interface at this depth by $1/e$. Using this criterion, the depth sampled for Cu K_α is on the order of 600 Å for $2\theta = 1.2°$ and on the order of 3200 Å for $2\theta = 12°$. The 2θ values are typical for first and fifth orders scattered from a 40-Å period film. Fits were made matching integrated intensities rather than peak intensities because the instrument broadens measured peaks.

The main observation we make for these data is that there is little change of the interfacial roughness, σ_{tot}, with N, i.e., the total film thickness. The value of σ_{tot} varied from 2.7 to 3.4 Å with no clear trend with N. If instead the first order is fit preferentially the average roughness ranges

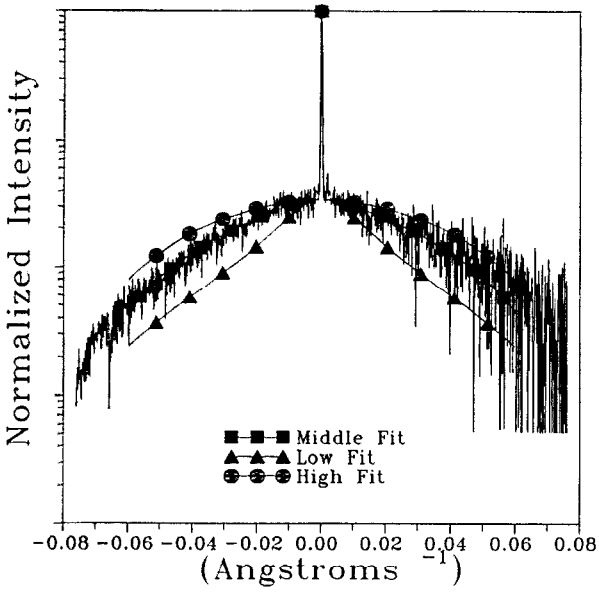

FIG. 3. A transverse (rocking) scan through the 5th order of the sample in 2(b) and theoretical fits bracketing the measurement. The solid triangles are calculated using $\alpha = \frac{1}{2}$, $\sigma_{corr} = 1.55$ Å, and $\xi = 80$ Å. The solid triangles are calculated using $\alpha = \frac{1}{2}$, $\sigma_{corr} = 2.2$ Å, and $\xi = 15$ Å. The solid squares (best fit) are calculated using $\alpha = \frac{1}{2}$, $\sigma_{corr} = 1.8$ Å, and $\xi = 30$ Å.

from 4.3 to 6.0 Å for these films, again with no clear trend versus N. The magnitude of Γ, the thickness of a W layer divided by the period thickness, is also determined from the fitting and for these films was ~ 0.51.

We used the fitting to explore the effect of choosing unequal roughness values for the W/C interfaces and the C/W interfaces. The main result of unequal roughness is to wash out the intensity modulation that arises due to Γ. For $\Gamma = 0.5$ and equal roughness even orders are suppressed. Unequal interfacial roughness builds up these suppressed intensities, particularly for the higher orders. For these films, fits show that the difference in roughness between the two types of interfaces can be no more than 0.5 Å. The effects of unequal roughness will be discussed in more detail in the next section.

In Fig. 3 we show an example of a transverse scan through the 5th diffraction order for the $N = 40$ sample of Fig. 3. The profile is made up of two components and is fit with the theory described previously. Fits varying σ_{corr} and ξ for $\alpha = \frac{1}{2}$ that bound the measured profile are plotted. We see that the fit is quite sensitive to the magnitude of the parameters.

We summarize the fitting results in Table I. The total interfacial roughness is observed to vary from sample to sample, but increased roughness is at best only slightly correlated with increasing N. A larger total roughness is associated with larger correlated roughness, suggesting that variations in substrate roughness replicated by the film may be the cause.

TABLE I. Summary of the results of fitting the specular reflectivity $(\theta,2\theta)$ curves and rocking curves for a series of W/C samples with a nominal bilayer period of $d = 40$ Å, varying the number of bilayers N. The results show only slight variations of the total interfacial roughness and the correlated interfacial roughness with N.

Sample	Description	σ total (Å)	σ corr. (Å)	ξ(Å)
B120790	$N = 10$, $d = 39.4$ $\Gamma = 0.515$	2.7	1.8	30
A041990	$N = 20$, $d = 37.1$ $\Gamma = 0.515$	2.7	1.7	80
B021291	$N = 40$, $d = 39.4$ $\Gamma = 0.51$	3.3	2.65	100
B112090	$N = 40$, $d = 38.2$ $\Gamma = 0.513$	2.7	1.85	45
A042490	$N = 40$, $d = 36.6$ $\Gamma = 0.513$	2.8	1.8	80
A042090	$N = 60$, $d = 37.4$ $\Gamma = 0.515$	2.8	1.85	100
A042390	$N = 80$, $d = 38.2$ $\Gamma = 0.515$	2.9	2.0	90
A021491	$N = 160$, $d = 38.9$ $\Gamma = 0.52$	3.4	2.6	100

B. Roughness versus period

In Fig. 4, we show $(\theta,2\theta)$ scans for films with $N = 40$ and a period d equal to 20, 80, and 160 Å. We also show a scan with $N = 10$, $d = 160$ Å. From the corresponding fits it is seen that the roughness of the $d = 20$ Å film falls in the range of that observed for the $d = 40$ Å films. The $d = 80$ Å film also falls in the range, but at the high end. The $d = 160$ Å films show a significant increase in roughness.

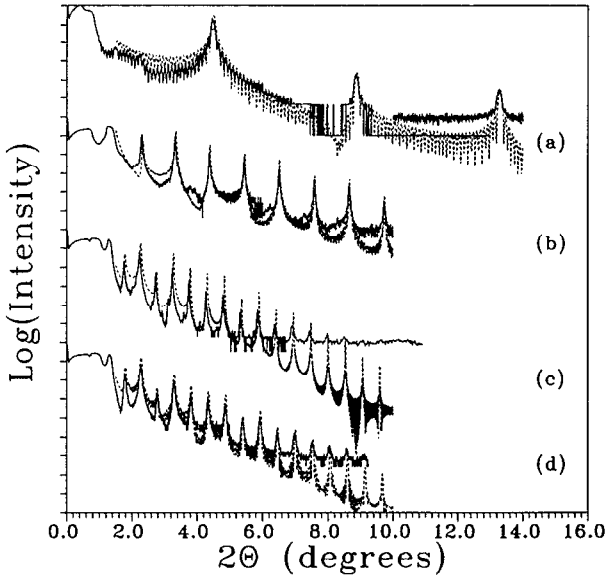

FIG. 4. A series of $(\theta,2\theta)$ scans and theoretical fits (dashed lines) for samples with varying periods. (a) $N = 40$, $d = 20.0$ Å, fit parameters: $\Gamma = 0.53$ and $\sigma_{tot} = 2.6$ Å. (b) $N = 40$, $d = 81.8$ Å, fit parameters: $\Gamma = 0.45$, $\sigma_{1tot} = 3.0$ Å, and $\sigma_{2tot} = 4.2$ Å. (c) $N = 40$, $d = 166$ Å, fit parameters: $\Gamma = 0.41$, $\sigma_{1tot} = 5.0$ Å, and $\sigma_{2tot} = 6.0$ Å. (d) $N = 10$, $d = 165$ Å, fit parameters: $\Gamma = 0.41$, $\sigma_{1tot} = 4.5$ Å, and $\sigma_{2tot} = 5.5$ Å. The scans in (c) and (d) show diffraction orders only to $2\theta < 9.9°$ consistent with their high interfacial roughness. Fits in (b)–(d) were obtained with alternate interfaces having different roughness values σ_{1tot} and σ_{2tot}.

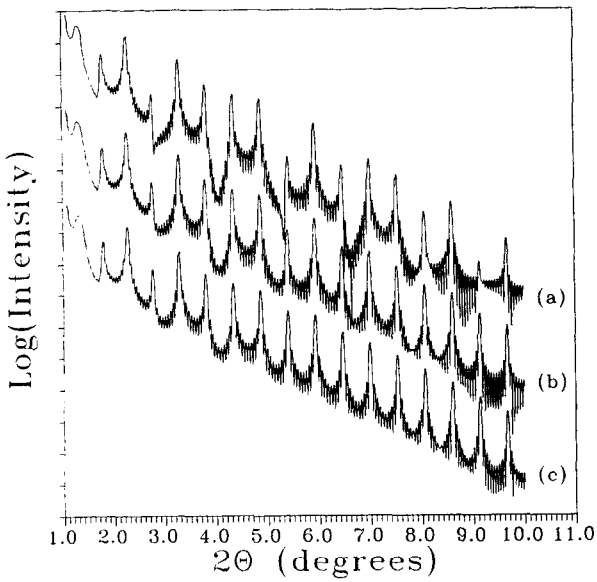

FIG. 5. A series of theoretical curves generated for $N = 10$, $d = 165$ Å, and $\Gamma = 0.41$ showing the effects of allowing the roughness of alternate interfaces to be unequal. (a) $\sigma_{1\text{tot}} = 4.8$, $\sigma_{2\text{tot}} = 4.8$, (b) $\sigma_{1\text{tot}} = 4.5$, $\sigma_{2\text{tot}} = 5.5$. (c) $\sigma_{1\text{tot}} = 4.2$, $\sigma_{2\text{tot}} = 6.5$. All three curves show a modulation of intensity due to Γ at the low orders. Increasing the difference in the roughness between alternate layers reduces the modulation preferentially at the higher orders.

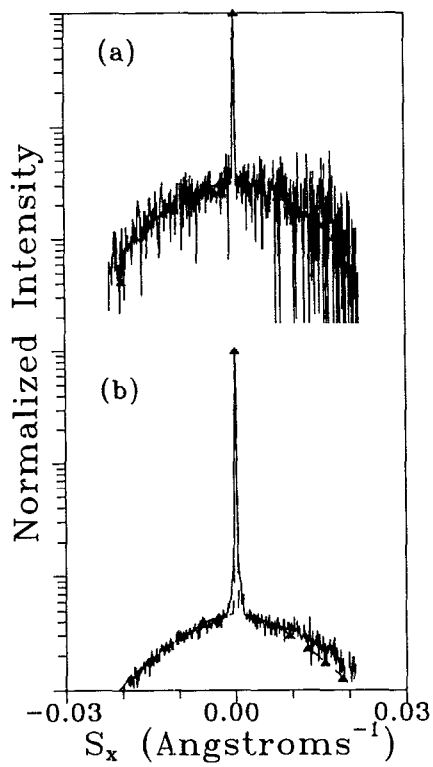

FIG. 6. Transverse scans and theoretical fits (solid triangles) showing the period dependence of the vertically correlated roughness. (a) $N = 10$, $d = 165$ Å, through the 12th-order peak ($2\theta = 6.452°$), best-fit parameters: $\alpha = \frac{1}{2}$, $\sigma_{\text{corr}} = 3.0$ Å, $\xi = 100$ Å. (b) $N = 40$ $d = 38.2$ Å, through the 3rd-order peak ($2\theta = 6.957°$), best-fit parameters: $\alpha = \frac{1}{2}$, $\sigma_{\text{corr}} = 1.6$ Å, and $\xi = 80$ Å. The two films have the same total thickness but the larger-period film shows significantly greater correlated roughness.

The fit was improved for the $d = 80$ and 160 Å data if interface roughness values for W/C ($\sigma_{1\text{tot}}$) and C/W ($\sigma_{2\text{tot}}$) were allowed to be unequal. In Fig. 5 we show a series of theoretical curves generated by varying the difference between W/C and C/W roughness for a $d = 160$ Å film. The main result is that increased differences wash out the modulation due to Γ, as previously discussed. We note that differences in roughness between alternate layers show up more readily when many diffraction orders are present.

In Fig. 6, we show transverse scans taken at similar values of S_z from $N = 10$, $d = 160$ Å and $N = 40$, $d = 40$ Å multilayers. It is seen that the diffuse background is significantly stronger in the $d = 160$ Å sample, implying that the vertically correlated roughness is also larger. The lateral correlation length is similar for both samples, showing no strong trend with period.

We summarize both the correlated and total roughness measurements for these samples in Table II. The main observation we make here is that both the absolute values of the vertically correlated roughness and the total roughness are significantly larger for the largest-period samples. We note that the relative interfacial roughness, the ratio σ_{tot}/d, decreases with increasing film thickness.

TABLE II. Summary of the results of fitting the specular reflectivity $(\theta,2\theta)$ curves and rocking curves for a series of W/C samples with fixed number of bilayers, $N = 40$, varying the bilayer period d and also samples with $N = 10$ and $d = 160$ Å. There is a trend of increased total interfacial roughness and increased vertically correlated roughness with increased bilayer period. The values of $\sigma_{1\text{tot}}$ and $\sigma_{2\text{tot}}$ represent the total roughness in alternate interfaces.

Sample	Description	σ total (Å) $\sigma_{1\text{tot}}$, $\sigma_{2\text{tot}}$	σ corr (Å)	ξ(Å)
A050790	$N = 40$, $d = 19.6$ $\Gamma = 0.53$	3.3, 3.3	2.5	90
A040390	$N = 40$, $d = 20.0$ $\Gamma = 0.54$	2.6, 2.6	1.4	50
A050290	$N = 40$, $d = 81.8$ $\Gamma = 0.45$	3.0, 4.2	2.0	110
A041790	$N = 40$, $d = 156$ $\Gamma = 0.41$	5.8, 7.0	4.9	175
B110691	$N = 40$, $d = 166$ $\Gamma = 0.41$	5.0, 6.0	4.5	60
A021391	$N = 10$, $d = 154$ $\Gamma = 0.41$	5.0, 6.0	4.0	100
A120790	$N = 10$, $d = 165$ $\Gamma = 0.41$	4.5, 5.5	3.1	90

C. Effect of a buffer layer

In Fig. 7, we show a $(\theta,2\theta)$ scan from an $N = 40$, $d = 40$ Å sample deposited on a 500-Å C buffer layer. In addition we show a scan from an $N = 40$, $d = 40$ Å sample deposited on a 400-Å C buffer layer deposited on a 20-Å W layer. Both show a large increase in roughness compared with the samples in Fig. 1. Only three diffraction orders are

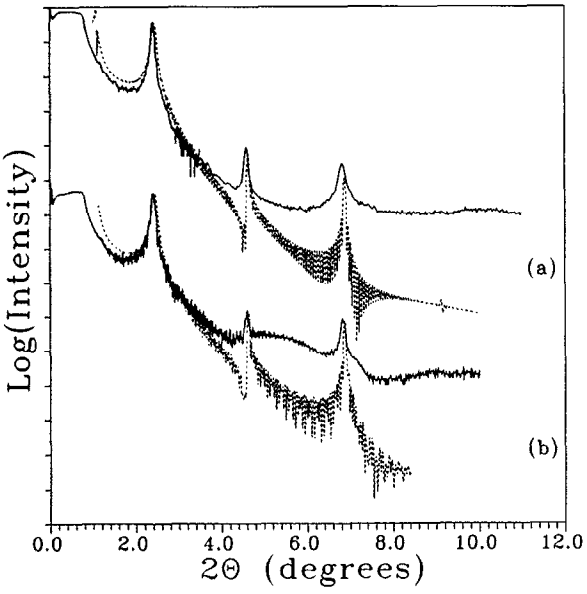

FIG. 7. Plots of $(\theta,2\theta)$ scans (solid) and theoretical fits (dashed lines) from a $N=40$, $d=40$ multilayer deposited on: (a) a 500-Å C buffer layer with $\sigma_{tot}=6.3$ Å and (b) a 400-Å C buffer layer on a 20-Å W layer with $\sigma_{tot}=5.5$ Å. Only three diffraction orders are observed as opposed to five in Fig. 2, as result of the increased interfacial roughness.

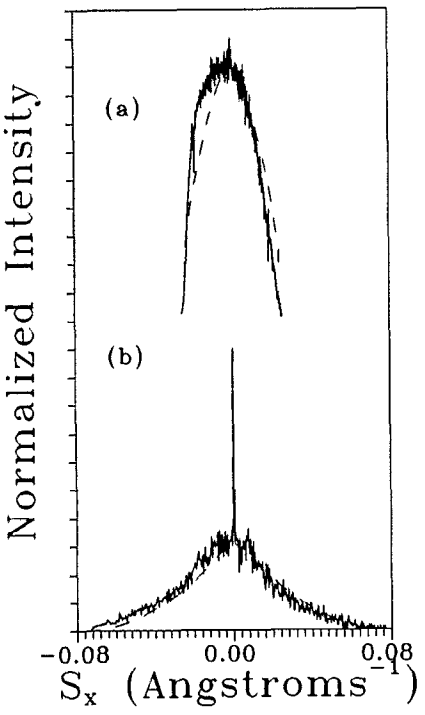

FIG. 8. Transverse scans and theoretical fits (dashed lines) through the 3rd-order peaks of the multilayers shown in Fig. 7. (a) 500-Å C buffer, best-fit parameters: $\alpha=\frac{1}{2}$, $\sigma_{corr}=5.9$ Å, and $\xi=200$ Å. (b) 400-Å C buffer layer on top of a 20-Å W layer, best-fit parameters: $\alpha=\frac{1}{2}$, $\sigma_{corr}=5.0$ Å, and $\xi=125$ Å. The intensity scale is linear. The diffuse background is large in both situations; in (a) the specular components of the scattered intensity is almost in the noise.

observable. The sample with the 500-Å buffer layers has the greater interfacial roughness. The large increase in total roughness is mirrored in an increase in the vertically correlated roughness as is shown by transverse profiles (Fig. 8) taken through the third diffraction orders that were plotted in Fig. 7. The specular component for the sample with the 500-Å C buffer layer is nearly gone. The sample with the 400-Å C layer has less correlated roughness but the diffuse intensity is still much larger than for corresponding samples with no buffer layer [Fig. 6(b)]. Note that Fig. 6 is a log scale while Fig. 8 is linear.

VI. DISCUSSION

We summarize here the main trends observed in this study. (1) Both the vertically correlated and total roughness are relatively independent of total film thickness in the range studied, 400 to 6400 Å, if the individual layer thickness is fixed (i.e., the number of bilayers, N, increases). (2) Both the vertically correlated roughness and the total roughness increase significantly when the thickness of layers increases while the total thickness is fixed. (3) The presence of a 500-Å sputter deposited C "buffer" layer greatly increases both correlated and total roughness in subsequently deposited multilayers. (4) The uncorrelated roughness changes much less than the correlated roughness for all samples. (5) The roughness difference between W/C and C/W interfaces is estimated to be on the order of 20%.

We begin by considering the dependence of interfacial roughness on total film thickness, i.e., on the number, N, of bilayers deposited for fixed individual layer thickness. For the thinnest sample, $[N=10]$, $\sigma_{tot}=2.7$ Å and for the thickest, $[N=160]$, $\sigma_{tot}=3.4$ Å. The evolution of roughness of a single film with thickness is expected to follow a growth law $W\propto t^{\beta}$, where w is the interface width (the rms roughness), t is the thickness, and β is the growth exponent. Various theoretical predictions of the growth exponent[16] range from $\frac{1}{4}$ to $\frac{1}{2}$. If one assumes that the variation in total roughness from 2.7 to 3.4 Å is real and uses the values in the interface roughness power law, one extracts an exponent of only ~ 0.1. This value is quite small and furthermore such a model cannot explain the dependence of the interfacial roughness on period or the effect of the buffer layer.

A second possibility is that there exists a source of roughness that is independent of the film thickness. This source could then obscure the component of roughness that increases with film thickness, giving an artificially low exponent. Two possible contributions to constant roughness are substrate roughness replicated through the film and uncorrelated roughness such as would arise due to the interdiffusion between consecutive layers. Variations in substrate roughness would appear as differences in the correlated roughness. For these samples correlated roughness behaves in the same way as total roughness, ranging from 1.8 to 2.6 Å for the same samples. The influence of interdiffused layers would show up in roughness uncorrelated from layer to layer, which can be estimated from the above using Eq. (6) and ranges from 2.0 to 2.2 Å. We see that

both contributions to the total roughness vary little, if at all, with N and that changes in σ_{tot} are accounted for with changes in σ_{corr}. The observed slight increase in σ_{tot} with N is within the range of values of σ_{tot} found in different films deposited with $N = 40$ and $d = 40$ Å, as shown in Table I, suggesting that variations in substrate roughness are the likely cause for the scatter in the data. Even though the existence of a total-thickness-independent component that masks a weak increase in total roughness could explain the N variation data, it cannot explain the large increase in roughness when the individual-layer thickness varies.

The most likely possibility is that the presence of the interfaces suppresses the increase in roughness that would occur if one were growing a single thick layer. One could imagine that at each interface the process for generating roughness would have to be restarted. This possibility implies that both the interface width and the lateral scale of the interfacial roughness depend primarily on the layer spacing and not the total film thickness, a result we suggest may be applicable to other multilayer composites. It also implies that kinetic growth roughness might be controlled with periodic thin "restarting layers."

The results of the C buffer layer support this conclusion. There is more carbon deposited in a multilayer than in the buffer layer. The initial C layer increases significantly the magnitude of both the total and the correlated roughness relative to the multilayer film without a buffer layer. This observation can be explained if the C layer is viewed as an initially rough substrate that is then copied by successive layers. The large increase in replicated roughness due to the presence of a C buffer layer confirms that roughness increases more rapidly in a single layer than for a similar amount deposited in a multilayer.

The marked dependence of the roughness on the individual-layer thickness is further evidence that roughness that develops during the growth of an individual layer (as opposed to purely replicated roughness) contributes strongly to the average interfacial roughness. Both the total interfacial roughness and the correlated roughness are increased for the 160-Å period films. It is possible that one layer type (i.e., either W or C) dominates in creating roughness. We know that C gets rougher and that W crystallizes for films thicker than ~40 Å. Hence, we expect that both contribute to the increasing roughness in thicker layers, but cannot at this time say which is more important.

How can we reconcile our proposal that the evolution of roughness is restarted in the growth of each successive layer with the observation that a significant portion of the roughness is vertically correlated? Consider the W and C are chemically quite different species. It is probable that the diffusion lengths of the two species on each other will differ. The species that can diffuse farther before being incorporated into the film may fill in the short-wavelength scale roughness of the opposing film, smoothening the layer. Continued deposition of these species will generate roughness with relatively long wavelengths. At the start of growth of the opposing species the substrate will appear flat on the short-wavelength scale. During the growth of this film some of the long-wavelength roughness will be copied while new, local, short-range roughness is generated. As this process proceeds with the deposition of additional layers the alternating smoothening and roughening processes will continue with the longer-wavelength roughness being propagated. This picture is, of course, highly idealized and can be complicated with the addition of other factors. These can include the possibility of interdiffusion between layers, the question of the wetting behavior of the deposited films (nonwetting coupled with some lateral mobility of the deposited atoms would cause clustering), and the question of the effects of energy distribution (for sputtered films) of the incoming atoms on the growth (massive atoms with high kinetic energy can penetrate into the matrix of the lighter material[29]).

VII. CONCLUSIONS

We have demonstrated that probing the intensity distribution of both specular and diffusely scattered x rays is a powerful way to characterize interfacial roughness and interfacial roughness correlation in multilayer films. We use a kinematic diffraction model of the transverse profiles (rocking curves) to extract both the magnitude and lateral correlation length of vertically correlated roughness for W/C films sputter deposited on Si(100) with varying thickness and periods. These measurements have given insight into the evolution of interfacial roughness. We propose on the basis of our results that the presence of the interfaces in a multilayer retard and/or modify the evolution of roughness that would occur in a film without interfaces.

Our measurements on thick C buffer layers, in addition to pointing out that C does not act as a smoothening layer, contrary to some previous work, suggest a new way to probe surface roughness. Instead of attempting to measure this surface roughness directly, either through synchrotron x-ray diffraction or with STM, it is possible to deposit a replicating multilayer structure on this film and measure the roughness as done here.

ACKNOWLEDGMENTS

This research has been supported by NSF, Solid State Chemistry Program, grant No. DMR 89-18927. We would like to thank R. Kariotis for useful discussions, T. Jankowski, J. Anderson, and R. Simon for growing the films, and T. Jankowski for help with the figures.

[1] For a review of soft x-ray multilayer mirrors including information on characterization, see T. W. Barbee Jr., SPIE **563**, 2 (1985).
[2] J. E. Harvey, W. P. Zmek, and E. C. Moran, SPIE **1160**, 209 (1989).
[3] Y.-H. Phang, D. E. Savage, T. F. Kuech, M. G. Lagally, J. S. Park, and K. L. Wang, Phys. Rev. Lett. (unpublished).
[4] See for example, Y. Lepêtre, E. Ziegler, and I. K. Schuller, Appl. Phys. Lett. **50**, 1480 (1987).
[5] P. Ruterana, J.-P. Chevalier, and P. Houdy, J. Appl. Phys. **65**, 3907 (1989).
[6] D. E. Savage, J. Kleiner, N. Schimke, Y.-H. Phang, T. Jankowski, J. Jacobs, R. Kariotis, and M. G. Lagally, J. Appl. Phys. **69**, 1411 (1991).
[7] P. Houdy, P. Boher, C. Schiller, P. Luzeau, R. Barchewitz, N. Alehyane, and M. Ouahabi, SPIE **948**, 95 (1988).

[8] For a review of surface roughness during growth see D. E. Wolf, in *Kinetics of Ordering and Growth at Surfaces*, edited by M. G. Lagally (Plenum, New York, 1990).
[9] R. Kariotis and M. G. Lagally, Surf. Sci. **216**, 557 (1989).
[10] A. Y. Cho, J. Appl. Phys. **42**, 2074 (1971).
[11] B. A. Movchan and A. V. Demchishin, Phys. Met. Metalorg. **28**, 83 (1969).
[12] J. A. Thornton, Ann. Rev. Mater. Sci. **7**, 239 (1977).
[13] See for example, R. Bruinsma, R. P. U. Karunasiri, and J. Rudnick, in *Kinetics of Ordering and Growth at Surfaces*, edited by M. G. Lagally (Plenum, New York, 1990).
[14] R. M. Messier and J. E. Yehoda, J. Appl. Phys. **58**, 3739 (1985).
[15] F. Family, J. Phys. A: Math. Gen **19**, L441 (1986).
[16] F. Family, to appear in the Proceedings of the Les Houches workshop on "Dynamical Phenomena at Surfaces, Interfaces, and Membranes," 1991.
[17] Summaries can be found in the articles contained in SPIE **563** (1985); **984** (1988); **1160** (1989).
[18] J. B. Kortright and J. D. Denlinger, Mater. Res. Soc. Symp. Proc. **103**, 95 (1988).
[19] G. M. Lamble, S. M. Heald, D. E. Sayers, E. Ziegler, and P. J. Viccaro, J. Appl. Phys. **65**, 4250 (1989).
[20] T. Oshino, D. Shindo, M. Hirabayashi, E. Aoyagi, and H. Nikaido, Jpn. J. Appl. Phys. **28**, 1909 (1989).
[21] A. K. Petford-Long, M. B. Stearns, C.-H. Chang, S. R. Nutt, D. G. Stearns, N. M. Ceglio, and A. M. Hawryluk, J. Appl. Phys. **61**, 1422 (1987).
[22] P. Boher, P. Houdy, and C. Schiller, J. Appl. Phys. **68**, 6133 (1990).
[23] B. G. Peterson, L. V. Knight, and H. K. Pew, SPIE **563**, 328 (1985).
[24] D. G. Stearns, J. Appl. Phys. **65**, 491 (1988).
[25] Y.-H. Phang, R. Kariotis, and M. G. Lagally (in preparation).
[26] S. K. Sinha, E. B. Sirota, S. Garoff, and H. B. Stanley, Phys. Rev. B **38**, 2297 (1988).
[27] In Ref. 6, we referred to the exponent α as h (see Ref. 26). Here we use α to be consistent with the roughness models described in Ref. 16.
[28] In Ref. 6, this equation contained a typographical error.
[29] W. L. Morgan and D. B. Boercker, Appl. Phys. Lett. **59**, 1176 (1991).